Use of artificial intelligence techniques to determine dental caries: A systematic review

Romany F. Mansour, Abdulsamad Al-Marghilnai and Zahar A. Hagas

***Abstract*—** Background: Dental caries is a chronic pathological condition affecting an estimated 36% of global population in their permanent teeth. It is characterized by demineralization of hydroxyapatite crystals and destruction of collagen matter in dental tissues. Various conventional methods for early detection of dental caries are used by dentists all over the world, such as Visible Light-Enhanced Techniques, Electronic Conductance Measurements, Electrical Impedance Spectroscopy, Digital radiography, Laser Fluorescence System and Ultrasound Caries Detector. However, the shortcomings of these techniques alarms the need to adopt a better method for early detection of caries.

Objective: The present study provides a systematic review of accuracy to use Raman spectroscopy as a method for caries detection at an early stage. Absence of sample penetration makes the method simple and hence is widely used.

Methodology: Significant information related to Raman spectroscopy has been extracted and utilized in the presentation of systematic review paper. Various parameters have been taken into account, such as type of Raman spectroscopy, central wavelength, optical power, description of the system, scan rate, description of Raman micro-spectroscopy, Raman imaging, Raman peak, Peak intensities of laser polarization direction, Depolarization ratio and polarization anisotropy.

Results and Discussion: The different research studies use varied system and central wavelength range that affects the result of each one of them. However, studies by M.T. Kirchner, et.al.(1997), Alex C.-T. Ko, et.al. (2006) and Alex C.-T. Ko, et.al. (2008) indicated maximum number Raman peak intensities corresponding to different functional groups, providing more information than other studies.

***Keywords*—** Dental caries, Artificial intelligence, Raman spectroscopy.

I. Introduction

Dental caries (Figure 1), a chronic disease, is a pathologic process that affects an estimated 36% of the population across the globe in their permanent teeth [1]. It is characterized by demineralization of inorganic substance (hydroxyapatite crystals) and destruction of organic substance (collagen matter) in dental tissues [2]. Two main factors are involved in the pathogenesis of dental caries: bacteria and diet. When the dietary source of sucrose is present, the cariogenic bacteria on the tooth surface ferments it to produce lactic acid. This lactic acid dissolves the hydroxyapatite crystals on the tooth surface leading to caries [3]. Although the prevalence of dental caries has fallen dramatically over the last few decades, its diagnosis still remains a challenging task.

Romany F. Mansour is with Department of Mathematics, Faculty of Science, New Valley, Assiut University, Egypt(email: romanyf@aun.edu.eg)
Abdulsamad Al-Marghilnai is with College of Computer Science & Information, Northen Border University, Saudi Arabia (email: srd.nbu@gmail.com)
Zahar A. Hagas is with Common First Year, King Saud University,Saudi Arabia (email : zahra@ksu.edu.sa)

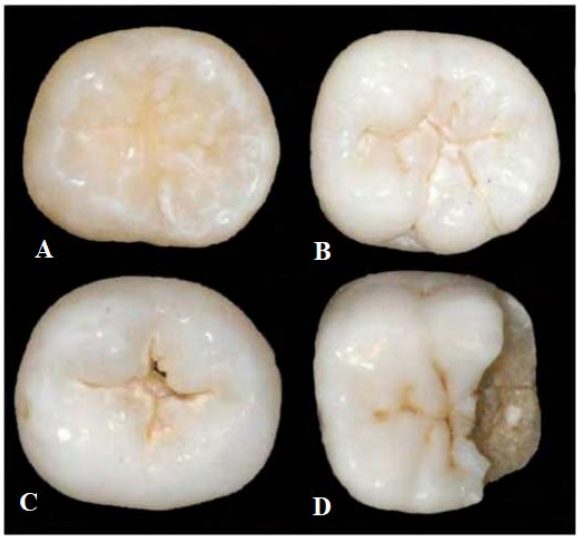

Fig. 1: (A) Sound occlusal surface. (B-D) Caries process in different stages [4].

A. Use of Artificial Intelligence in medical studies

The human intelligence processes such as learning, reasoning and self-correction, when incorporated in computer systems constitute simulations, termed as Artificial Intelligence (AI). Today, when AI is looked over for various worldly ambitions, healthcare applications rank top in funding in last few years with use of Machine Learning (ML) [5]. With excitement in the investor and research communities, many ML industry startups are making efforts to healthcare, significantly. Researchers across the globe have come up with various applications of ML and also claim for future applications which are gaining momentum with appropriate funding and research focus [6].

B. Current machine learning applications in healthcare

Disease Identification and diagnosis- In 2015, a report by Pharmaceutical Research and Manufacturers of America stated that 800 ML generated anti-cancer medicines and vaccines

were in trial [7]. Also, IBM Watson Health, in 2016, declared their partnership with Quest Diagnostics for IBM Watson Genomics. The aim of this initiative was the use of integrating cognitive computing and genomic tumor sequencing to make decision in medicine making [8], [9]. Another initiative called Google's DeepMind Health was developed to address muscular degeneration in aging eyes [10].

Medical Imaging- Diagnosis is a complicated process and involves various factors. InnerEye initiative started in 2010 by Microsoft is currently used as image diagnostic tool. With deep learning, more data sources contribute to AI diagnostic process and hence diagnostic applications become more accessible [11]–[16].

Medical data collection- For the treatment of Parkinson's disease and Asperger's syndrome, ResearchKit by Apple allows users to access apps that evaluates their condition over time. IBM's partnership with Medtronic handles data of diabetes and insulin in real time and is going to great lengths to acquire health data [17].

Drug Discovery- Drug discovery is the emerging healthcare application using ML, with relatively straightforward economic value. IBM and Google have now started emerging in drug discovery and now being a part various host companies that are raising and making money with ML in the field of drug discovery [18][19].

Robotic Surgery- Major attention in the field of robotic surgery has been given to da Vinci robot that allows surgeons to manipulate dexterous robotic limbs. This device performs surgeries with fine details than human hand alone. Some systems involve computer vision, in order to identify distances or minute body parts [20].

Various applications of ML are gaining momentum for future applications with help of today's funding and research focus. These may involve- personalized medicines depending on the patient's medical history, genetic lineage, past conditions, diet, and stress level; automatic treatment or recommendation using a machine that could adjust a patient's dose of medications by tracking their blood profile, diet, sleep, and stress; autonomous master robotic surgeries [5].

II. Literature Review

A. Existing methods to detect dental caries

Dental caries is a dynamic process which involves episodes of de-mineralization of enamel soon after tooth eruption. The conventional methods to detect the caries include visual inspection, tactile sensation and radiographs [21].

Consequently, various other detection systems have emerged in the recent years. The Visible Light- Enhanced Techniques work on the principle of light scattering. These techniques contain three main systems of early carious detection that use different sources of light: FOTI (Fiber-Optic Trans-illumination), QLF (Quantitative Light-Induced Fluorescence) and DiFOTI (Digital Image Fiber-Optic Trans-illumination). While FOTI (Figure 2a) is used for detection of proximal caries, QLF (Figure 2c & 2d) is majorly used for diagnosing a range of lesions and provides evidence as most promising technology to detect caries, as it provides advantage of detecting caries in closer correlation with changes in mineral content. Another method, Electronic Conductance Measurements (ECM) (Figure 3) uses fixed frequency (23 Hz) alternating current to monitor the dental caries detection including the presence and extent of caries, either from enamel or exposed dentine surface [22]. This method provides the results as bulk resistance of tooth tissue. The device consists of a probe, a substrate and metal bar. The probe acts as a source of current, while the tooth typically serves the purpose of substrate.

A metal bar, contra-electrode, is held in patient's hand. Some physical parameters such as the temperature of the tooth, tissue thickness and material hydration affect the ECM results. Alternatively, a similar application, Electrical Impedance Spectroscopy (EIS) scans a range of electrical frequencies and provides results in the form of capacitance and impedance. Digital radiography (Figure 4) is an enhanced diagnostic technique which is as reliable as conventional methods. Radiographic subtraction is a method in this regard, which is based on the principle comparing two radiographs of same object using their pixel values. It is a promising technique to detect caries and assessment of bone loss. Detection of occlusal decay is also done using DIAGNOdent (DD) (Figure 2b), a Laser Fluorescence System. DD is incorporated with a 655 nm diode laser that can detect non-cavitated, occlusal pit-and-fissure caries at an early stage. This method provides a numerical value on two LED display, which is related to the suitability of restoration. Besides these techniques, Ultrasound Caries Detector (UCD) systems are capable of discriminating cavitated and non-cavitated lesions. The major advantage of this technique lies in the reduced exposure of patient to ionizing radiation. Many studies have documented that UCD had higher sensitivity than the radiographs in diagnosis of proximal caries [23].

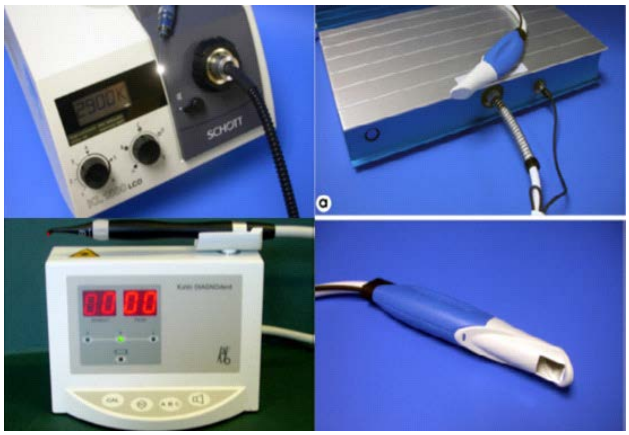

Fig. 2: (a)FOTI Equipment; (b) DIAGNOdent device; (c & d) QLF Systems [24].

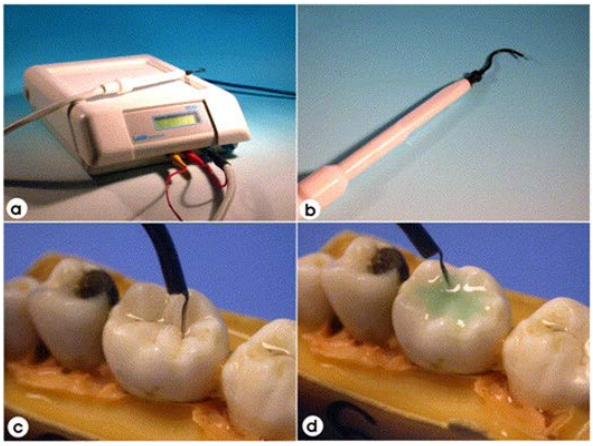

Fig.3: (a) ECM device and its application; (b) the machine; (c) the hand piece; (d) site specific measurement technique; surface specific measurement technique [24]

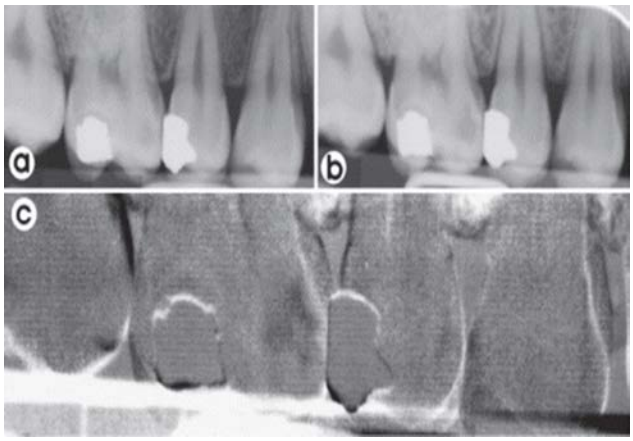

Figure 4: Example of a subtraction of two digital bitewing radiographs. (a) Radiograph showing proximal lesion on mesial surface of first molar; (b) follow up radiograph taken 12 months later; (c) the areas of difference between the two films are shown as black, i.e. in this case the proximal lesion has become more radiolucent and hence has progressed [24]

In recent years, Raman spectroscopy showed promising results in the detection of early dental caries. As stated already, the dental caries is portrayed by demineralization of hydroxyapatite crystals. Raman spectroscopy helps in characterization of hydroxyapatite crystals ($Ca_{10}(PO_4)_6(OH)_2$) [25][26]. Figure 5 demonstrates Raman spectroscopy of sound enamel and carious enamel.

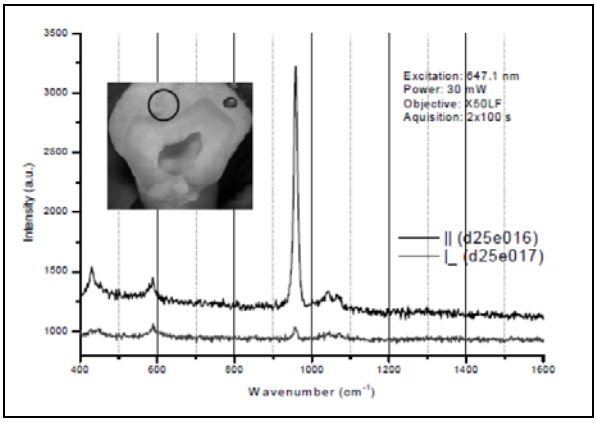

Figure 5: Raman spectroscopy of sound and carious enamel (Adapted from Ionita 2009)

B. Shortcomings in the existing methods

Each of the conventional methods used for detection of dental caries have various limitations and disadvantages. High intensity visible lights used in Visible Light-Enhanced Visual Techniques can cause reflection of light over the tooth surface, underlying dentine shade, and saliva layer refraction [27][28]. Moreover, penetration of light photons through dense hydroxyapatite disruptions. Laser Fluorescence Measurement has been ineffective in early detection of enamel defects due to small or inaccessible diagnostic probe [24]. Although digital radiographs have been effective in identifying different stages of decay, yet they are not reliable to detect caries at an early stage [28]. Additionally, inability of DD to determine the depth of lesions proved that fluorescence-based intra-oral devices cannot be considered as better devices for early carious detection [29]–[33].

C. Need for artificial intelligence in detecting dental caries

Research in the recent past has established that a majority of dental caries are unable to be identified in routine examination including x-rays. While occlusal caries is easy to identify through a normal clinical examination or x-ray review, yet these detection methods are not reliable for a large percentage of caries, such as those below the surface of the tooth, interproximal caries, and root caries.

An AI company, ParallelDots, Inc., started a cloud based AI application for cavity detection on dental x-rays. They named this new clinical device as Dentistry.AI [34]. The device contains thousands of bitewing radiographic images, that act as data set. In order to recognize patterns from these large data sets, AI algorithm is trained. The advantage of AI is its exposure to numerous data which improves its efficiency to perform a specific task [35].

AI makes better identification of caries by analyzing bone density. Correctly interpreting X-rays and 3D images requires a lot of experience, and AI assistant makes the job much easier as it has already viewed a millions of images. It holds the applications in caries detection, implants, periodontics and orthodontics. AI algorithm trained with thousands of X-rays attains a high level of accuracy in predicting the location of caries. This system is now being tested by dentists in clinics in investigational device study. Several such AI algorithms may be developed in order to provide better accuracy to dentists to detect early caries at a specific location [36].

D. Challenges in using AI for detecting dental caries

The major shortcoming of a trained deep learning system is its limited data set in comparison to ever increasing dental problems. Furthermore, the pathway it follows to provide the results is unknown, i.e. regardless of its accuracy the AI device does not explain "how" it made the predictions. This problem is more challenging for dentist, where they won't want to suggest surgical procedure to the patients without a firm understanding of how the device arrived at its recommendation.

E. Aim of Work

In the present study, we attempted to systematically review the accuracy of data for caries detection using Raman spectroscopy.

This method is currently widespread because of its simplicity due to the absence of sample preparation. Contrastingly, IR spectroscopy requires laborious sample preparation. In the beginning, when Raman spectroscopy was acknowledged in the biomedical field for early caries diagnosis, a few disadvantages such as fluorescence from the organic tissues and absence of sensitive instrument were the major concerns. In the last decade, progresses in the advancement of Raman spectroscopy have increased significantly when contrasted with IR spectroscopy. All modifications that have been made in Raman spectroscopic imaging till now are specifically aimed to determine peaks in spectrum. These peaks can be further used as finger prints to distinguish the carious tissues to normal tissues. Various studies have identified that Raman spectra at 959 cm-1 was able to identify the extent of demineralization [25][37].

III. Research Methodology

A. Search Strategy

Different electronic databases were searched to do the relevant literature survey for the present systematic review. The databases that were investigated involved PubMed, EMBASE, and Wiley Online Library pertaining to the time frame of last 37 years until present; 15th May 2018.

For the purpose of performing the literature search the following set of single or combined keywords were used: Dental caries, Artificial intelligence, AI, Machine learning, ML, Raman spectroscopy, early detection of dental caries, identification of dental caries, Raman, dental, caries, detection.

B. Description of Inclusion and Exclusion Criteria

The inclusion and exclusion criteria for a particular study depend on the type of research studies to be included or excluded for systematic review. The various parameters that were important for our present study included the following inclusion and exclusion criteria: language of research papers, availability of full text articles, and type of interventions (Raman spectroscopy) to be used; conventional methods used for the early detection of dental caries; advantages and shortcomings of AI systems; sample size; and the types or modifications made to Raman Spectroscopy.

1) Inclusion Criteria

The below-mentioned set of inclusion criteria was designated to collect relevant information from various research studies fulfilling the aim of our present research:

- Clinical research papers published in English language;
- All the relevant studies were considered from the year 1980 till 2017;
- Literature involving early detection of dental caries;
- Papers that specify the sample size used for the study;
- Papers that contain clear description of the type of Raman spectroscopy used for carious detection;
- Studies that have reported various parameters of Raman spectroscopy used for a particular study, such as central wavelength, optical power, system description, peak intensities and laser polarization or depolarization values;
- Studies that report the advantages and shortcomings of AI systems for early detection of caries were included;
- Research papers that present the findings of dental caries.

2) Exclusion Criteria

The various exclusion criteria used to reduce inclusion of non-pertinent information sources were:

- Foreign language published articles and half articles
- Studies that use the existing AI techniques to identification of dental caries
- Unavailability of data, such as type of clinical study and polarization/depolarization anisotropy data;
- Studies that lack detailed information on parameters used in Raman spectroscopy for their research;
- Reviews, meta-analysis, Systematic reviews, thesis and dissertations, letters, editorials, abstracts, unpublished studies, case reports, and small case series are rejected.

C. Selection of studies

The initial search performed using the search strategy produced 575 results from various databases. Further, exclusion of articles that were presented in language other than English, those that did not contain information about Raman spectroscopy, or systematic review and meta-analysis papers, thesis and dissertation, etc. led to final number of 72 articles. From these 72 articles, 50 relevant studies were selected for screening. Exclusion of articles from these was based on unavailability of full-text articles, and duplicate studies. Full-text articles that were found to be eligible for the present systematic review were a count of 43, from which 28 others were eliminated due to incomplete data or unrelated information. Finally, in order to understand the effectiveness of Raman spectroscopy in early detection of dental caries, a total of 15 out of these 43 research studies were studied for the present review. The details of the study selection are demonstrated as a flowchart in Figure 6.

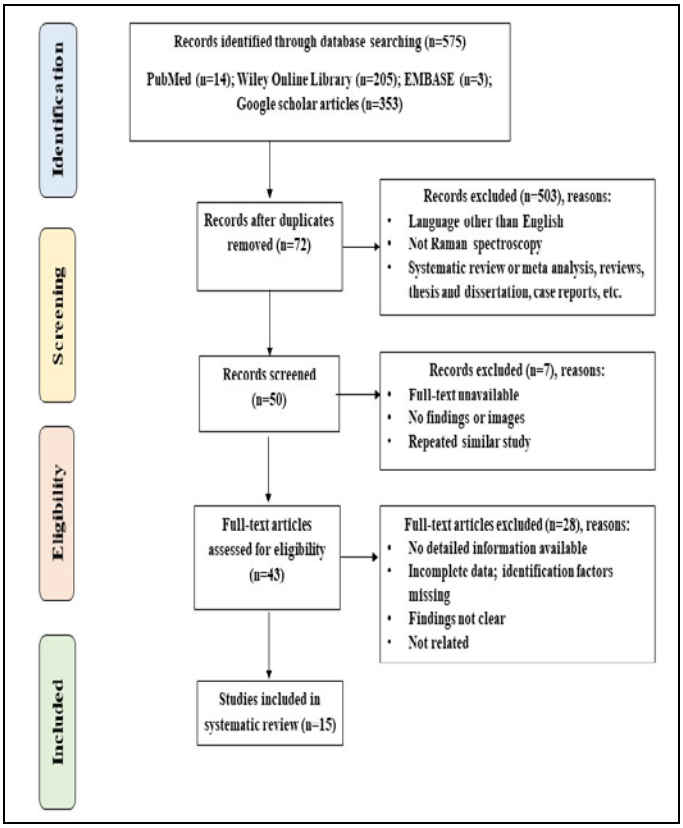

Fig. 6: Flowchart of study selection.

D. Data Extraction

The research papers presented with significant information pertaining to Raman spectroscopy utilized in the research study and various parameters related to it. The following information was found to be important based on literature assessment and hence, these parameters were considered from each study: author's name, year of publication, tooth samples, type of Raman spectroscopy, central wavelength, optical power, description of the system, scan rate, description of Raman micro-spectroscopy, Raman imaging, Raman peak, and Peak intensities of laser polarization direction. Furthermore, depolarization ratio and polarization anisotropy data of both sound enamel and carious lesion were also extracted. Due to distraction in structure of enamel, depolarization ratio provides information about vibrational mode assignment, and polarization anisotropy deviates the light path. This gives a clue for presence of dental caries and further diagnosis can be performed. However, due to unavailability of complete information in research articles, these parameters could not be used for analysis process.

IV. Systematic Review

The data for systematic review was extracted in order to understand the pros and cons of early detection of dental caries using different types of Raman Spectroscopy. Table 1 shows the characteristics of the studies included in the present systematic review, wherein the data included 15 studies in the time frame of 1980-2018.

We observe that various types of Rama n Spectroscopic techniques have been used to detect early dental caries including, FT-Raman Spectra, Diode laser Raman spectroscopy, Optical coherence tomography, Polarized Raman spectroscopy, micro-Raman spectroscopy, Fibre-optic coupled polarized Raman spectroscopy, Renishaw 'inVia' Raman microscope, and dispersive Raman spectrometer.

Apart from the parameters that have been described in Table 1, the depolarization ratio was observed in the range of 0.05 to 18, whereas these limits increased for carious lesions, with least depolarization ratio of 0.4. On the other hand, a decreasing trend in polarization anisotropy was observed when dental caries was detected, in comparison to sound enamel.

DECLERATION

Ethics approval and consent to participate No ethics approval or consent to participate was needed for this work, as it did not involve direct human material, human subjects or human data. Consent for publication No consent for publication was needed for the data used in this work. Competing interests the authors declare that they have no competing interests.

Availability of data materials: Not applicable Funding: This study was not funded

Conflict of Interest: No conflict of interest exists

Informed consent: Informed consent was obtained from all individual participants included in the study.

Authors' contributions: The present study provides a systematic review of accuracy to use Raman spectroscopy as a method for caries detection at an early stage. Absence of sample penetration makes the method simple and hence is widely used. Significant information related to Raman spectroscopy has been extracted and utilized in the presentation of systematic review paper. Various parameters have been taken into account, such as type of Raman spectroscopy, central wavelength, optical power, description of the system, scan rate, description of Raman micro-spectroscopy, Raman imaging, Raman peak, Peak intensities of laser polarization direction, Depolarization ratio and polarization anisotropy. All authors read and approved of the final manuscript.

Acknowledgements: There are no further acknowledgements beyond the ones already stated above.

V. CONCLUSION

The different research studies use varied system and central wavelength range that affects the result of each one of them differently. M. T. Kirchner et.al. (1997) reported that Quantitative measurements of organic to inorganic ratio can be determined from FT-Raman spectroscopy, in order to study the changes in dentine due to burial conditions. Different burial conditions must be tested for accurate analysis. This technique can thus be employed for analysis of not just whole teeth but may also be used for study of a fragment of tooth. Wieland Hill et.al. (2000) concluded from their study that carious lesions can be distinguished from sound hard tooth tissues using the difference in their near-IR Raman spectra. The near-IR Raman spectra of carious tooth shows increased luminescence. Diode laser Raman spectroscopy has therefore proved to be efficient, fast and reliable method for detection of caries. Alex C.-T. Ko (2006) based their results, to discriminate sound enamel from carious lesion, on the difference between degree of Raman polarization anisotropy. Carious lesions produce decreased Raman polarization anisotropy or inversely high depolarization ratio. These results depend on 2 factors- scattering and degree of hydroxyapatite crystal orientation. This study provides the relevant data and major aspects of Raman spectroscopy. It claims to help in formulation of dental treatment plans as well as monitoring of lesion based on fluoride treatment during re-mineralization process. Michael G. Sowa et.al. (2006) also observed Raman depolarization ratio of the same intensity as by Alex C.T. Ko et.al. (2006). The technique demonstrated significant difference in depolarization ratio of sound and carious enamel. Measurements of depolarization ratio, attenuation coefficient and OCT provide better understanding and detection of caries at an early stage. Fiona Gilchrist et.al. (2007) supported their Raman spectroscopic data with scanning electron microscopy. This confirmed that these two techniques can be together used to understand the presence or absence of eroded carious lesions on the primary and secondary teeth specimen. The study provides significance of the technique to analyze mineral concentration in teeth. Alex C.-T. Ko et.al. (2008) reported that fibre-optic coupled polarized Raman spectroscopy is an effective tool to detect dental caries at an early stage. This technique provides a single spectrum with complete of information about parallel as well as cross-polarized Raman spectra simultaneously. The method is highly sensitive and its specificity in micro-spectroscopic analysis makes it a better tool than other methods. Hamideh Salehi et.al. (2012) demonstrated the emergence of fluorescence variation of dental caries and reported that no significant correlation was observed between Raman spectra characteristics, fluorescence variation and HPLC assay. B. Mohanty et.al. (2012) provided results stating that surface layer may lead to less chances of detection demineralized sub-surface region. This study presents a limitation of using Raman spectroscopy for early detection of dental cavities. Another study by A. Almahdy et.al. (2011) provided an evidence that the non-invasive technique of micro-Raman spectroscopy can detect caries in different dentine zones, without unnecessary tissue removal procedure. B Coello et.al. (2015) demonstrated the clinical reliability of quantitative Raman spectroscopy by examining two case studies, which successfully identified demineralized dental tissues. Fabíola Bastos de Carvalho et.al. (2013) presented a comparative study of DIAGNOdent and Raman spectroscopic data for detection of carious lesions, and further reported that Raman spectroscopy is a better and more sensitive technique, as it identifies changes in inorganic components of tooth samples. T. Buchwald et. al. (2017) analyzed three independent phenomena, i.e. Raman scattering, Rayleigh scattering and fluorescence emission for detection of caries. They presented Raman spectroscopy as a new diagnostic tool for detection of carious lesions.

Raman spectroscopic data has proved in all these studies to effective for various reasons. First of all, minimal or no sample preparation is required for detection of caries using Raman spectroscopy. Second, studies by M.T. Kirchner, et.al.(1997), Alex C.-T. Ko, et.al. (2006) and Alex C.-T. Ko, et.al. (2008)

indicated maximum number Raman peak intensities corresponding to different functional groups, hence providing more information than other studies, described above. Also, these studies provide a better understanding of Raman spectroscopic data to detect dental caries. However, each of these methods require further in vitro analysis.

REFERENCES

[1] K. Yadav and S. Prakash, "Dental Caries: A Review," *Asian J. Biomed. Pharm. Sci.*, vol. 6, no. 53, pp. 01–07, 2016.

[2] P. V Seredin and V. N. Melkumov, "Research Hydroxyapatite Crystals and Organic Components of Hard Tooth Tissues Affected by Dental Caries Using Ftir-Microspectroscopy and XRD-Microdiffraction," *World Appl. Sci. J.*, vol. 31, no. 12, pp. 2101–2107, 2014.

[3] P. W. Caufield and A. L. Griffen, "Dental Caries: An infectious and Transmittable Disease," *Pediatr. Clin. North Am.*, vol. 47, no. 5, pp. 1001–1019, Oct. 2000.

[4] M. Baffi Diniz, J. De, A. Rodrigues, and A. Lussi, "Traditional and Novel Caries Detection Methods," in *Contemporary Approach to Dental Caries*, Ming-Yu Li, Ed. InTech, 2012, pp. 105–128.

[5] Daniel Faggella, "Machine Learning Healthcare Applications - 2018 and Beyond," *TechEmergence*, 2018. [Online]. Available: https://www.techemergence.com/machine-learning-healthcare-applications/.

[6] L. S. Coles, "The application of artificial intelligence to medicine," *Futures*, vol. 9, no. 4, pp. 315–323, Aug. 1977.

[7] Pharmaceutical Research and Manufacturers of America, "Medicines in development for Cancer-a report on Cancer," 2015.

[8] Memorial Sloan Kettering Cancer Center, "IBM Watson and Quest Diagnostics Launch Genomic Sequencing Service Using Data from MSK Share Print," 2016. [Online]. Available: https://www.mskcc.org/ibm-watson-and-quest-diagnostics-launch-genomic-sequencing-service-using-data-msk.

[9] IBM, "IBM Watson Health - Cognitive Healthcare Solutions," 2016. [Online]. Available: https://www.ibm.com/watson/in-en/health/.

[10] DeepMind, "DeepMind Health and research collaborations," 2016. [Online]. Available: https://deepmind.com/applied/deepmind-health/working-partners/health-research-tomorrow/.

[11] Y. Ioannou *et al.*, "Decision Forests, Convolutional Networks and the Models in-Between," *Microsoft Res. Tech. Rep.*, Mar. 2016.

[12] C. Morrison *et al.*, "Assessing Multiple Sclerosis With Kinect: Designing Computer Vision Systems for Real-World Use," *Human–Computer Interact.*, vol. 31, no. 3–4, pp. 191–226, Jul. 2016.

[13] J. Margeta, A. Criminisi, R. Cabrera Lozoya, D. C. Lee, and N. Ayache, "Fine-tuned convolutional neural nets for cardiac MRI acquisition plane recognition," *Comput. Methods Biomech. Biomed. Eng. Imaging Vis.*, vol. 5, no. 5, pp. 339–349, Sep. 2017.

[14] B. H. Menze, Z. W. Tu, G. Langs, and A. Criminisi, *Medical Computer Vision. Recognition Techniques and Applications in Medical Imaging*, vol. 6533. Berlin, Heidelberg: Springer Berlin Heidelberg, 2011.

[15] E. Geremia, B. H. Menze, O. Clatz, E. Konukoglu, A. Criminisi, and N. Ayache, "Spatial Decision Forests for MS Lesion Segmentation in Multi-Channel MR Images," in *Medical Image Computing and Computer-Assisted Intervention*, 2010, pp. 111–118.

[16] A. Hosny, C. Parmar, J. Quackenbush, L. H. Schwartz, and H. J. W. L. Aerts, "Artificial intelligence in radiology," *Nat. Rev. Cancer*, vol. 2018, pp. 1–11, May 2018.

[17] Apple (IN), "ResearchKit and CareKit- Empowering medical researchers, doctors and you." [Online]. Available: https://www.apple.com/in/researchkit/.

[18] Simon Smith, "The 'Watson' Era of Machine Learning in Drug Discovery is Over—Now We're in the Long Tail," 2017. [Online]. Available: https://blog.benchsci.com/machine-learning-in-drug-discovery-long-tail.

[19] Reportlinker, "Deep Learning in Drug Discovery and Diagnostics, 2017 - 2035," 2017. [Online]. Available: https://www.prnewswire.com/news-releases/deep-learning-in-drug-discovery-and-diagnostics-2017---2035-300433645.html.

[20] Intuitive Surgical Inc., "da Vinci Surgery | Robotic-Assisted Surgery," 2015. [Online]. Available: http://www.davincisurgery.com/.

[21] D. McComb and L. E. Tam, "Diagnosis of occlusal caries: Part I. Conventional methods," *J. Can. Dent. Assoc. (Tor).*, vol. 67, no. 8, pp. 454–457, 2001.

[22] M. Huysmans, C. Longbottom, A. Christie, P. Bruce, and R. Shellis, "Temperature dependence of the electrical resistance of sound and carious teeth," *J. Dent. Res.*, vol. 79, no. 7, pp. 1464–1468, 2000.

[23] S. Matalon, O. Feuerstein, and I. Kaffe, "Diagnosis of approximal caries: bite-wing radiology versus the Ultrasound Caries Detector: An in vitro study.," *Oral Surg Oral Med Oral Pathol Oral Radiol Endod*, vol. 95, pp. 626–631, 2003.

[24] K. Parveen, "Methods for Caries Detection : an Overview," *Pakistan Oral Dent. J.*, vol. 35, no. 4, 2015.

[25] A. C. Ko, L. P. Choo-Smith, M. Hewko, M. G. Sowa, C. C. Dong, and B. Cleghorn, "Detection of early dental caries using polarized Raman spectroscopy," *Opt Express*, vol. 14, pp. 203–215, 2006.

[26] A. C. Ko, L. P. Choo-Smith, M. Hewko, L. Leonardi, M. G. Sowa, and C. C. Dong, "Ex vivo detection and characterization of early dental caries by optical coherence tomography and Raman spectroscopy," *J Biomed Opt*, vol. 10, 2005.

[27] S. K. Choksi, J. M. Brady, D. H. Dang, and M. S. Rao, "Detecting Approximal Dental Caries with Transillumination: A Clinical Evaluation," *J. Am. Dent. Assoc.*, vol. 125, no. 8, pp. 1098–1102, Aug. 1994.

[28] A. Schneiderman, M. Elbaum, T. Shultz, S. Keem, M. Greenebaum, and J. Driller, "Assessment of Dental Caries with Digital Imaging Fiber-Optic Transllumination (DIFOTI^{TM}): In vitro Study," *Caries Res.*, vol. 31, no. 2, pp. 103–110, 1997.

[29] D. A. Tagtekin *et al.*, "Caries detection with DIAGNOdent and ultrasound," *Oral Surgery, Oral Med. Oral Pathol. Oral Radiol. Endodontology*, vol. 106, no. 5, pp. 729–735, Nov. 2008.

[30] X.-Q. Shi, S. Tranaeus, and B. Angmar-Månsson, "Validation of DIAGNOdent for quantification of smooth-surface caries: an in vitro study," *Acta Odontol. Scand.*, vol. 59, no. 2, pp. 74–78, Jan. 2001.

[31] A. Lussi, S. Imwinkelried, N. B. Pitts, C. Longbottom, and E. Reich, "Performance and Reproducibility of a Laser Fluorescence System for Detection of Occlusal Caries in vitro," *Caries Res.*, vol. 33, no. 4, pp. 261–266, 1999.

[32] T. F. Novaes, C. M. Moriyama, M. S. De Benedetto, E. K. Kohara, M. M. Braga, and F. M. Mendes, "Performance of fluorescence-based methods for detecting and quantifying smooth-surface caries lesions in primary teeth: an *in vitro* study," *Int. J. Paediatr. Dent.*, vol. 26, no. 1, pp. 13–19, Jan. 2016.

[33] A. Theocharopoulou, M. D. Lagerweij, and A. J. van Strijp, "Use of the ICDAS system and two fluorescence-based intraoral devices for examination of occlusal surfaces.," *Eur. J. Paediatr. Dent.*, vol. 16, no. 1, pp. 51–5, Mar. 2015.

[34] Dentistry.AI, "AI Powered Caries Detection," *Dentistry.AI*. [Online]. Available: https://www.dentistry.ai/.

[35] Shashank Gupta, "Automated Caries Detection on Bitewing Radiographs Using Deep CNNs," *ParallelDots*, 2017. [Online]. Available: https://blog.paralleldots.com/research/automated-caries-detection-bitewing-radiographs-using-deep-cnns/.

[36] D. Lou Shuman and A. P. & A. Singh, "The AI revolution that's coming to dentistry," *Dent. Prod. Rep.*, Mar. 2018.

[37] M. Miyazaki, H. Onose, and B. K. Moore, "Analysis of the dentin-resin interface by use of laser Raman spectroscopy," *Dent Mater*, vol. 18, pp. 576–580, 2002.

Table 1 shows the characteristics of the studies included in the present systematic review.

	Study Details	Tooth Samples	Type of Raman spectroscopy used	Central wavelength	Optical power	Description of the system	Description of the Raman Microspectroscopy	Raman Imaging	Raman peak intensities (cm-1)	Peak Intensities of laser polarization direction
1	M.T. Kirchner, *et.al.*1997	9	FT-Raman Spectra were obtained with Bruker IFS66 infrared instrument	1064 nm	200-500 mW	FRA106 Raman module attachment	Fourier transform Raman Spectroscopy was used to obtain the Raman spectra. Sample excitation was effected with Nd:YAG laser operating at 1064 nm.	Spectral resolution of 4 cm-1	590 cm-1, 430 cm-1, 1667 cm-1, 1451 cm-1, 1245 cm-1	590 cm-1, 430 cm-1
2	Wieland Hill, *et.al.* 2000	10	Diode laser Raman spectroscopy consisting of biomedical Raman proble for in vivo measurements	785 nm	30 mW	Fiber-optic probe (Kaise optical systems, HFPF-785)	Diode laser spectra containing diode laser, a wavelength of 785 nm and maximm power of 350 mW	5 X 1 s acquistion time	500 cm-1, 960 cm-1,1050 cm-1	930 cm-1, 960 cm-1
3	Alex C.-T. Ko, *et.al.* 2006	13	Optical coherence tomography image slices were acquired on an OCT-2000 system with software Revision A	850 nm	750 µW	NIR (780-1250 nm range) linear polarizer	Near-infrared laser excitation at 830 nm, laser beam profiles of 100 mW and 500 mW power at the laser head at 830 nm, laser power at the sample was measured to be 12 mW and 40 mW, 10x lens,	55 µm steps, 17 x 14 array map covering an area of 880 x 715 µm2,	590 cm-1, 608 cm-1, 959 cm-1, 1069 cm-1 and 1104 cm-1	959 cm-1 (phosphate ions); 1104 cm-1 (carbonate ion);
4	Michael G. Sowa, *et.al.*2006	16	Polarized Raman spectroscopy on on a LabRamHR confocal Raman microspectrometer.	830 nm	12 mW	Polarized Raman spectra were acquired on a LabRamHR confocal Raman microspectrometer (HORIBA Jobin-Yvon, Edison, NJ, USA) operating with near-infrared laser excitation at 830 nm (Lynx series TEC 100, Sacher Lasertechnik GmbH, Marburg, Germany).	Polarized Raman instrumentation and the tooth sampling geometry were used.LabSpec (ver. 4.12) software bundled with the LabRamHR system was used for spectrometer control and data acquisition.Measurements were acquired with a Nikon ×10 microscope objective with laser powers of approximately 12 mW.	6.5 min		960 cm-1(phosphate ions)
5	Fiona Gilchrist, *et.al.* 2007	10	micro-Raman spectroscopy (MRS) by monochromatic laser	632.8 nm	20 mW	Spectra were obtained from all specimens using a 20-mW red laser	micro-Raman equipment with A silicon specimen,with a characteristic band at 520.8 cm, was used to	1-µm steps along the linear areas	520 cm-1, 958.5 cm-1, 967 cm-	958 cm-1 and 967 cm-1

	Study Details	Tooth Samples	Type of Raman spectroscopy used	Central wavelength	Optical power	Description of the system	Description of the Raman Microspectroscopy	Raman Imaging	Raman peak intensities (cm-1)	Peak Intensities of laser polarization direction
			excitation			(HeNe) with a wavelength of 632.817 nm, combined with a slit of 150 µm, a confocal hole of 250 µm and a 1800 mm g−1 holographic grating.	calibrate the computer software program linked to the LabRam 300 (Horiba Jobin Yvon).		1	
6	Alex C.-T. Ko, *et.al.* 2008	47	Fibre-optic coupled polarized Raman spectroscopic system.	830 nm	300 mW	Axial raman spectrograph equipped with a CCD camera	A fibre-optic coupled polarization-resolved Raman spectroscopic system optmized for 830nm excitiation.	1 sec integration time with 10 acquisitions and 90 mW laser illumination power	431 cm-1, 590 cm-1, 609 cm-1, 959 cm-1 and 1070 cm-1	959 cm-1
7	I Ionita 2008	10	Raman microspectrometer T64000 HORIBA Jobin Yvon,	647.1 nm	30 mW	Raman microspectrometer T64000 HORIBA Jobin Yvon, operating with the 647.1 nm excitation line from an Ar+ -Kr+ laser (Coherent Innova-70) and confocal microscope Olympus (objective ×50LF).	Raman instrumentation with the addition of a NIR (780-1250 nm range) linear polarizer (Edmund Optics, Blackwood, NJ, USA) at the exit of the laser radiation and a NIR polarization analyzer placed after the notch filter.	objective ×50LF	959 cm-1	959 cm-1(phosphate ions)
8	Hamideh Salehi, *et.al.*2012	2	Raman spectra with LabRAM ARAMIS IR2 confocal micro-Raman spectrometer	632.8 nm	12 mW	micro-Raman spectrometer with 1800 grooves per mm grating	Micro-Raman spectrometer equipped with BX41 Olympus microscope. Spectra obtained with 632.8 nm radiation from He-Ne laser.	90s with 3 accumulations	433 cm-1, 579 cm-1, 959 cm-1, 1071 cm-1	959 cm-1 (phosphate ions); 1103 cm-1 (carbonate ion);
9	B. Mohanty, *et.al.* 2012	6	micro-Raman spectroscopy with Renishaw inVia Raman	785 nm		Raman microscope with 785nm laser and a grating of 1200 lines/mm	The laser used was focused with Leica DMLM 20X objective with a spatial resolution of less than 1 µM.	40 acquisitions with each acquisition 5µm	300-2000 cm-1	520 cm-1(phosphate ions); 1070cm-1

	Study Details	Tooth Samples	Type of Raman spectroscopy used	Central wavelength	Optical power	Description of the system	Description of the Raman Microspectroscopy	Raman Imaging	Raman peak intensities (cm-1)	Peak Intensities of laser polarization direction
			microscope					apart		(carbonate ion);
10	Almahdy, F.C, *et.al.* 2012	8	Renishaw 'inVia' Raman microscope (Renishaw Plc) in StreamLine TM scanning mode	785 nm	100 mW	Raman spectra of each tooth was scanned using a 785-nm diode laser (100 mW sample power) through a X 20/0.40 NA air objective	Raman signal was acquired using a 600-lines/mm grating centred between 849 and 1,603 cm –1 and 2 s CCD exposure time. The spectral resolution was 8.55 cm –1. For each tooth, around 400,000 spectra were recorded	600- lines/mm	849 cm-1,1603 cm-1	960 cm-1(phosphate ions); 1340 cm-1 CO3)
11	Fabíola Bastos de Carvalho, *et.al.* 2013	20	dispersive Raman spectrometer (AndorShamrockSR303i)	655 nm	500 mW	dispersive Raman spectrometer (AndorShamrockSR303i ; Andor Technology, Belfast, Northern Ireland) and a stabilized diode laser (λ = 785 nm, 500 mW; B & W TEK, Newark, DE, USA)	Raman spectra was performed by a fiber optic cable (Raman Probe) positioned in contact with the samples. The band used for analysis ranged from 200 to 1800 cm-1. Detection of scattered light signal of the sample was done by a back-illuminated thinned, deep depletion (1024x128" pixels) iDUS CCD camera (Andor Technology)		575 cm-1,960 cm-1,1450 cm-1	960 cm-1(phosphate apatite ions) 575 cm-1 (fluoridated apatite ions)
12	Fabíola Bastos de Jose Luis Gonzalez-Solıs, *et.al.* 2014	39	Jobin-Yvon LabRAM HR800 Raman Spectrometer	830 nm	17 mW	Jobin-Yvon LabRAM HR800 Raman Spectrometer with a laser of 830-nm wavelength was used.	The Raman system was calibrated with a silicon semiconductor using the Raman peak at 520 cm−1. All spectra were taken and collected in the region from 200 to 1,800 cm−1, with a resolution of 0.6 cm−1.	×50 objective	520 cm-1	CO2− 3 (240–300 cm−1), CaF2 (322 cm−1), PO3− 4 ν2 vibrations (437 and 450 cm−1), PO3− 4 ν1 vibrations (960 cm−1), PO3− 4 ν3 vibrations (1,045 cm−1), and

	Study Details	Tooth Samples	Type of Raman spectroscopy used	Central wavelength	Optical power	Description of the system	Description of the Raman Microspectroscopy	Raman Imaging	Raman peak intensities (cm-1)	Peak Intensities of laser polarization direction
										CO2− 3 ν1 vibration (1,073 cm−1)
13	B Coello, *et.al.* 2015	8	Raman spectroscopy with FT Raman Bruker RFS100 and OPUS software	1064 nm	1500 mW	Nd:YAG (neodymium-doped yttrium aluminium garnet) laser (1064 nm)	Raman spectra were collected by using a FTRaman Bruker RFS 100 equipped with a Nd:YAG (neodymium-doped yttrium aluminium garnet) laser (1064 nm) with incident laser radiation up to 1500 mW.		575 cm-1, 960 cm-1, 1450 cm-1	430 cm-1(phosphate ions); 960cm-1 (hydroxypatite);
14	Pavel Seredin, *et.al.* 2015	10	Raman and fluorescence microspectroscopy in backscattering geometry	514.5 nm	40 mW	Raman spectra with laser excitation power of 40 mW and argon laser with λ = 514.5 nm	Raman spectra included a close-cycle He cryostat, a TRIAX550 monochromator, and a liquid-nitrogen-cooled charge-coupled-device (CCD) detector (Princeton Instruments). The laser beam was focused on the sample using a x50 microscope objective	10 seconds	775 cm-1, 1075 cm-1, 1115 cm-1	410 cm-1(phosphate ions); 959cm-1 CO3)
15	Tomasz Buchwald, *et.al.* 2017	10	inVia Renishaw micro-spectrometer were used to detect several parameters such as intensity, position or FWHM of Raman band	785 nm and 514.5 nm	30 mW	diode-pumped laser and argon laser	Raman scattering spectra measurements were carried out with two lasers emitting 785nm and 514.5 nm. Excitation of laser power at 30 mW and 3 mV	100 μm steps analysed in an area of 3500 X 3000 μm2	959 cm-1	959 cm-1